Particle motion in the Einstein-Euler-Heisenberg rotating black hole spacetime

Daniel Amaro,[1,2,*] Claus Lämmerzahl,[1,†] and Alfredo Macías[2,‡]

[1]*ZARM, University of Bremen, Am Fallturm, 28359 Bremen, Germany*
[2]*Physics Department, Universidad Autónoma Metropolitana–Iztapalapa, PO. Box 55–534, C.P. 09340, CDMX, México*

(Received 12 March 2023; accepted 7 April 2023; published 25 April 2023)

We study the motion of charged test particles and photons in the gravitational field of the rotating electrically charged Einstein-Euler-Heisenberg black hole solution. This describes a nonlinear electromagnetic generalization of the Kerr-Newman solution, which endows the vacuum with an effective dielectric constant. The orbits of photons are analyzed by means of the effective Plebański pseudometric related to the geometrical metric and to the electromagnetic energy-momentum tensor. The QED induced modifications of the shape of the shadow are presented and discussed.

DOI: 10.1103/PhysRevD.107.084040

I. INTRODUCTION

Quantum electrodynamical (QED) vacuum corrections to the Maxwell-Lorentz theory can be accounted for by an effective nonlinear theory of the electromagnetic field derived by Euler and Heisenberg (EH) [1,2] using the Dirac electron-positron theory. Schwinger reformulated this result within a gauge invariant formulation of QED [3]. When the electric fields are stronger than the critical value, $D_c \equiv m^2c^3/(e\hbar)$, spontaneous electron-positron pair production takes place, lowering the vacuum energy. The vacuum is treated as a specific type of medium, the polarizability and magnetizability properties of which are determined by clouds of virtual charges surrounding the real currents and charges [4]. This effect can be interpreted as an effective dielectric constant of the vacuum. This theory is a valid physical theory [5], and a possible direct measurement of the EH induced effects has been proposed by Brodin *et al.* [6].

The gravitational collapse of a star to a Kerr-Newman (KN) black hole, with all the aspects of nuclear physics and electrodynamics involved is a complex problem in astrophysics [7]. Astrophysical black holes are more likely to be neutral, but during gravitational collapse there is expected to be a process of charge separation, when the gravitational energy of the collapsing core is transformed into electromagnetic energy and eventually in electron-positron pairs created by vacuum polarization. Such QED effects have been studied by Ruffini *et al.* [8–11] in the powering mechanism of gamma-ray bursts by means of black hole energy extraction and using observational data. The observation of stars, in particular of the S2 star, around SgrA* [12] as well as the direct observation of gravitational waves [13] give overwhelming evidence for the existence of black holes. Moreover, also the observations of a shadow of the compact object at the center of the galaxy M87 as well as SgrA* at the center of the Milky Way reported in 2019 and 2022, respectively, by the Event Horizon Telescope team [14] are perfectly explained through the existence of black holes.

Ruffini *et al.* [15] considered the contributions of the EH effective Lagrangian in order to formulate the Einstein-Euler-Heisenberg theory (EEH) and studied the static spherically symmetric black hole solutions endowed with electric and magnetic charges. They reduced the problem to screened Reissner-Nordström solutions, where the nonlinear corrections were collected in the screening terms of the electromagnetic charges. Another approach was studied by Yajima *et al.* [16], in which the EH Langrangian is considered as the low-energy limit of the Born-Infeld theory [17], and the nonlinearity parameters are treated as free parameters.

Plebański introduced a class of nonlinear electrodynamic theories [18], which contains Born-Infeld and EH nonlinear electrodynamics (NLED) as special cases [4]. In the framework of the EEH theory, Amaro *et al.* [19] derived an electrically charged static black hole solution in terms of the Plebański dual variables and studied the trajectories of test particles and the shadow of the black hole. Furthermore, Bretón *et al.* [20] followed the QED interpretation of Ruffini *et al.* [15] for obtaining the screened KN black hole solution. They used the ansatz for a Kerr-like metric and for the electromagnetic Plebański dual variables, considered the symmetries for Petrov type-D metrics, and solved the Einstein equations. The nonlinearity introduces virtual

*daniel.amaro@zarm.uni-bremen.de
†laemmerzahl@zarm.uni-bremen.de
‡amac@xanum.uam.mx

charges that lead to a screening of the real charges and also affect the geometry of the underlying spacetime.

In this paper we first analyze how the EH modifications affects the charged particle motion: we also consider a screened charge for the test particle and discuss the resulting structure of the effective potential for its motion. Second, we study photon propagation in the spacetime endowed with EH NLED as well as the modifications of the shape of the shadow of the black hole. The outline of the paper is as follows: in Sec. II, the EEH theory and its formulation in terms of the dual Plebański variables are revisited. In Sec. III, the EEH rotating electrically charged black hole solution is reviewed. In Sec. IV, the charged particle motion is studied. In Sec. V, the light geodesics and the shadow of the black hole are analyzed. Finally, the summary and conclusions of the work are presented in Sec. VI.

II. THE EINSTEIN-EULER-HEISENBERG THEORY

We revisit the basic features of the Einstein theory coupled with the EH NLED [1] in the formalism introduced by Plebański [18]. The action for Einstein gravity minimally coupled to a linear or nonlinear Maxwell theory reads [1,21]

$$W = \frac{1}{16\pi G}\int_{M_4} d^4x\sqrt{-g}R + W_{\mathrm{M}}(X,Y), \tag{1}$$

where R is the Ricci curvature scalar, g the determinant of the metric $g_{\mu\nu}$, and G the Newton's constant, which we will take $G=1$. The variables X and Y are the only two independent relativistic invariants constructed from the Maxwell field in four dimensions, i.e.,

$$X = \frac{1}{4}F_{\mu\nu}F^{\mu\nu}, \qquad Y = \frac{1}{4}F_{\mu\nu}{}^{*}F^{\mu\nu}. \tag{2}$$

$F_{\mu\nu} = \partial_\nu A_\mu - \partial_\mu A_\nu$ is the Faraday tensor and A_μ the electromagnetic four potential. Its dual is defined as ${}^{*}F^{\mu\nu} = \frac{1}{2\sqrt{-g}}\epsilon^{\mu\nu\sigma\rho}F_{\sigma\rho}$, with $\epsilon_{\mu\nu\sigma\rho}$ being the completely antisymmetric tensor that satisfies $\epsilon_{\mu\nu\sigma\rho}\epsilon^{\mu\nu\sigma\rho} = -4!$. The components of $F_{\mu\nu}$ are the electric field $\mathbf{E}$, and the magnetic field strength $\mathbf{B}$. Then the two invariants read $X = (\mathbf{E}^2 - \mathbf{B}^2)/2$ and $Y = -\mathbf{E}\cdot\mathbf{B}$.

In the case of a EH NLED we have

$$W_{\mathrm{M}} = \frac{1}{4\pi}\int_{M_4} d^4x\sqrt{-g}\left(-X + \frac{2\alpha^2}{45m_e^4}\{4X^2 + 7Y^2\}\right), \tag{3}$$

where m_e is the electron mass and α the fine structure constant.

The EH field equations derived from this action (1) are more easily written in terms of the Legendre dual description of NLED [18], which involves the introduction of the Plebański tensor $P_{\mu\nu}$ defined by

$$dL(X,Y) = -\frac{1}{2}P^{\mu\nu}dF_{\mu\nu}, \tag{4}$$

where $L(X,Y)$ is the Lagrangian density for the NLED. In general it is given by

$$P_{\mu\nu} = -(L_X F_{\mu\nu} + L_Y {}^{*}F_{\mu\nu}), \tag{5}$$

where subscripts on L denote differentiation. The Plebański tensor $P_{\mu\nu}$ coincides with the Faraday tensor $F_{\mu\nu}$ for the linear Maxwell theory. In our case it reads

$$P_{\mu\nu} = F_{\mu\nu} - \frac{4\alpha^2}{45m_e^4}\{4XF_{\mu\nu} + 7Y{}^{*}F_{\mu\nu}\}. \tag{6}$$

The components of $P_{\mu\nu}$ are given by the electric field strength $\mathbf{D}$ and the magnetic field $\mathbf{H}$. Accordingly, (6) can be interpreted as constitutive or material relations of the EH NLED.

We denote by $\tilde{s}$ and $\tilde{t}$ the two independent invariants in terms of the dual Plebański variables $P_{\mu\nu}$

$$\tilde{s} = -\frac{1}{4}P_{\mu\nu}P^{\mu\nu}, \qquad \tilde{t} = -\frac{1}{4}P_{\mu\nu}{}^{*}P^{\mu\nu}, \tag{7}$$

where the dual tensor is given by ${}^{*}P^{\mu\nu} = \frac{1}{2\sqrt{-g}}\epsilon^{\mu\nu\sigma\rho}P_{\sigma\rho}$. In terms of $\mathbf{D}$ and $\mathbf{H}$ the two invariants read $\tilde{s} = (\mathbf{D}^2 - \mathbf{H}^2)/2$ and $\tilde{t} = -\mathbf{D}\cdot\mathbf{H}$. The structural function $H(\tilde{s},\tilde{t})$ is given by

$$H(\tilde{s},\tilde{t}) = -\frac{1}{2}P^{\mu\nu}F_{\mu\nu} - L, \tag{8}$$

which for the EH theory (up to terms of higher order in α) reduces to

$$H(\tilde{s},\tilde{t}) = \tilde{s} - \frac{2\alpha^2}{45m_e^4}\{4\tilde{s}^2 + 7\tilde{t}^2\}. \tag{9}$$

To obtain the original variables we use the constitutive relations

$$F_{\mu\nu} = H_{\tilde{s}}P_{\mu\nu} + H_{\tilde{t}}{}^{*}P_{\mu\nu} = P_{\mu\nu} - \frac{16\alpha^2}{45m_e^4}\left[\tilde{s}P_{\mu\nu} + \frac{7}{4}\tilde{t}{}^{*}P_{\mu\nu}\right], \tag{10}$$

where the subscripts on H denote differentiation.

The equations of motion for the EEH theory are the Faraday, the Maxwell, and the Einstein equations [22]:

$$d{}^{*}F = 0, \qquad dP = 0, \qquad R_{\mu\nu} - \frac{1}{2}Rg_{\mu\nu} = 8\pi T_{\mu\nu}, \tag{11}$$

with the energy-momentum tensor

$$T_{\mu\nu} = \frac{1}{4\pi}[H_{\tilde{s}} P_\mu{}^\beta P_{\nu\beta} + g_{\mu\nu}(2\tilde{s}H_{\tilde{s}} + \tilde{t}H_{\tilde{t}} - H)]. \tag{12}$$

$F_{\mu\nu}$ and ${}^*P_{\mu\nu}$ are curls and then can be written as a gradient of an electromagnetic potential. The energy-momentum tensor for the EH NLED is given by

$$T_{\mu\nu} = \frac{1}{4\pi}\left[\left(1 - \frac{16\alpha^2}{45m_e^4}\tilde{s}\right)P_\mu{}^\beta P_{\nu\beta} + g_{\mu\nu}\left(\tilde{s} - \frac{2\alpha^2}{45m_e^4}\{12\tilde{s}^2 + 7\tilde{t}^2\}\right)\right]. \tag{13}$$

III. ROTATING EINSTEIN-EULER-HEISENBERG BLACK HOLE

The rotating electrically charged EEH black hole solution has been derived in [20]. Using the ansatz for a Kerr-like spacetime with the EH NLED as a source, the obtained spacetime appears as a screened KN solution.

In Boyer-Lindquist coordinates, the potential of the electromagnetic part of EEH for the dual Plebański variables is given by the ansatz

$$B = B_\alpha dx^\alpha = -\frac{Qa\cos\theta}{\Sigma}\left(dt - \frac{(r^2+a^2)}{a}d\phi\right). \tag{14}$$

The dual Plebański 2-form ${}^*P = dB$ reads

$$\begin{aligned} {}^*P = &\frac{2Q}{\Sigma^2}ar\cos\theta dr \wedge (dt - a\sin^2\theta d\phi) \\ &+ \frac{Q}{\Sigma^2}(r^2 - a^2\cos^2\theta)\sin\theta d\theta \wedge [adt - (r^2+a^2)d\phi]. \end{aligned} \tag{15}$$

The components satisfy the relations ${}^*P_{r\phi} = a\sin^2\theta {}^*P_{tr}$ and $a{}^*P_{\theta\phi} = (r^2+a^2){}^*P_{t\theta}$. The Plebański 2-form is

$$\begin{aligned} P = &\frac{Q}{\Sigma^2}(r^2 - a^2\cos^2\theta)dr \wedge (dt - a\sin^2\theta d\phi) \\ &+ \frac{Q}{\Sigma^2}ar\sin 2\theta d\theta \wedge [(r^2+a^2)d\phi - adt]. \end{aligned} \tag{16}$$

The components are also related by $P_{r\phi} = a\sin^2\theta P_{tr}$ and $aP_{\theta\phi} = (r^2+a^2)P_{t\theta}$. From (7) the invariants $\tilde{s}$ and $\tilde{t}$ reduce to

$$\tilde{s} = \frac{Q^2}{2\Sigma^2} - \frac{4\mathcal{M}^2 r^2\cos^2\theta}{\Sigma^4}, \tag{17}$$

$$\tilde{t} = \frac{2Qr\cos\theta}{\Sigma^4}\mathcal{M}(r^2 - a^2\cos^2\theta), \tag{18}$$

where the rotationally induced magnetic moment $\mathcal{M} = Qa$ was introduced [23].

Since the components B_μ are given by (14), then we can compute the components A_μ of the electromagnetic potential, using the constitutive relations (10). These equations relate $P_{\mu\nu}$ and ${}^*P_{\mu\nu}$ with $F_{\mu\nu} = \partial_\nu A_\mu - \partial_\mu A_\nu$, and differ from those for the linear Maxwell case. Hence, the following solution for $A = A_\nu dx^\nu$ can be derived

$$\begin{aligned} A = &\left\{1 - \frac{10\alpha}{225\pi}D_Q^2 + \frac{10\alpha}{225\pi}H_Q^2 + \frac{60\alpha}{225\pi}H_Q^2\frac{H_Q^2}{D_Q^2}\right\} \\ &\times \frac{Qr}{\Sigma}[dt - a\sin^2\theta d\phi], \end{aligned} \tag{19}$$

where the square of the radial components of the electromagnetic fields read

$$D_Q^2 = \frac{Q^2}{\Sigma^2 D_c^2}, \qquad H_Q^2 = \frac{\mathcal{M}^2\cos^2\theta}{\Sigma^3 D_c^2}, \tag{20}$$

where $D_c = m_e^2c^3/(e\hbar)$ is the critical field, and where we used the relation $16\alpha^2/(45m_e^4) = 20\alpha/(225\pi D_c^2)$. For $\alpha = 0$, the usual electromagnetic potential for the KN black hole solution is recovered.

Moreover, only two contravariant components of the energy-momentum tensor $T^{\mu\nu}$ for the EH NLED (13) are independent

$$8\pi T^{rr} = -\frac{\Delta Q^2}{\Sigma^3}\left(1 - \frac{16\alpha^2}{45m_e^4}\tilde{s}\right) - \frac{16\alpha^2}{45m_e^4}\frac{\Delta}{\Sigma}\left(\tilde{s}^2 + \frac{7}{4}\tilde{t}^2\right), \tag{21}$$

$$8\pi T^{\theta\theta} = \frac{Q^2}{\Sigma^3}\left(1 - \frac{16\alpha^2}{45m_e^4}\tilde{s}\right) - \frac{16\alpha^2}{45m_e^4}\frac{1}{\Sigma}\left(\tilde{s}^2 + \frac{7}{4}\tilde{t}^2\right), \tag{22}$$

while, due to the underlying symmetry [20], the rest of the nonvanishing components are linear combinations of these [20]:

$$T^{tt} = -\frac{(r^2+a^2)^2}{\Delta^2}T^{rr} + a^2\sin^2\theta T^{\theta\theta}, \tag{23}$$

$$T^{t\phi} = -\frac{(r^2+a^2)a}{\Delta^2}T^{rr} + aT^{\theta\theta}, \tag{24}$$

$$T^{\phi\phi} = -\frac{a^2}{\Delta^2}T^{rr} + \frac{1}{\sin^2\theta}T^{\theta\theta}. \tag{25}$$

According to the QED interpretation of the EH NLED, the vacuum polarization acts as clouds of virtual charges screening the real electric charge and thus the rotationally induced magnetic moment, affecting the geometry only through the screened values of the real charges [15]. Therefore, in [20] the effects of the vacuum polarization are nearly constant and affect only the electric charge of the EH NLED as in flat spacetime [7]. The solution to the

Einstein field equations is the rotating EEH black hole spacetime

$$
\begin{aligned}
ds^2 = &-\left(1 - \frac{2Mr - \tilde{Q}^2}{\Sigma}\right) dt^2 + \frac{\Sigma}{\Delta} dr^2 \\
&- \frac{(2Mr - \tilde{Q}^2) 2a \sin^2\theta}{\Sigma} dt d\phi + \Sigma d\theta^2 \\
&+ \left(r^2 + a^2 + \frac{(2Mr - \tilde{Q}^2) a^2 \sin^2\theta}{\Sigma}\right) \sin^2\theta d\phi^2, \\
\Sigma = &\; r^2 + a^2 \cos^2\theta, \\
\Delta = &\; r^2 + a^2 - 2Mr + \tilde{Q}^2, \qquad (26)
\end{aligned}
$$

which represents a screened KN-like black hole. The screened charge of the black hole is defined as

$$
\begin{aligned}
\tilde{Q}^2 = Q^2 \Bigg\{ 1 - \frac{5\alpha}{225\pi} \Bigg[D_Q^2 - 4H_Q^2 \left(1 - \frac{a^2 \cos^2\theta}{\Sigma}\right) \\
\times \left(7 - 12 \frac{a^2 \cos^2\theta}{\Sigma} + 12 \frac{a^4 \cos^4\theta}{\Sigma^2}\right) \Bigg] \Bigg\}. \qquad (27)
\end{aligned}
$$

From the condition $\Delta = 0$, the event horizon r_+ and the inner horizon r_- are given by

$$
r_\pm = M \pm \sqrt{M^2 - a^2 - \tilde{Q}^2}, \qquad (28)
$$

which is an example of a quantum effect changing the geometry, as mentioned above. The ergoregion is the region $r_+ < r < r_{\rm st}$ between the event horizon and the static limit surface $r_{\rm st}$ defined by

$$
r_{\rm st} = M + \sqrt{M^2 - \tilde{Q}^2 - a^2 \cos^2\theta}. \qquad (29)
$$

Hence, the features of a KN black hole are recovered, but with a screened black hole charge (27). The static screened Reissner-Nordström solution is recovered for $a = 0$ [19].

IV. TRAJECTORIES OF CHARGED TEST PARTICLES

The Lagrangian for a charged test particle which interacts with an electric field is given by [24]

$$
\mathcal{L} = \frac{1}{2} g_{\mu\nu} \dot{x}^\mu \dot{x}^\nu - q A_\mu \dot{x}^\mu, \qquad (30)
$$

where q is the electric charge of the test particle, and the dot denotes differentiation with respect to the affine parameter τ. Its coupling with the electromagnetic field is exactly the same in NLED [18]. The Hamiltonian is given by the Legendre transformation $\mathcal{H} = \pi_\mu \dot{x}^\mu - \mathcal{L}$, with the canonical momentum $\pi_\mu = g_{\mu\nu} \dot{x}^\nu - q A_\mu$. It reads [23]

$$
\mathcal{H} = \frac{1}{2} g^{\mu\nu} (\pi_\mu + q A_\mu)(\pi_\nu + q A_\nu). \qquad (31)
$$

Since it does not depend explicitly on τ, it is a constant of motion, $\mathcal{H} = -\mu^2/2$, determined by the normalizing condition, i.e., $\mu^2 = -g_{\mu\nu} \dot{x}^\mu \dot{x}^\nu = 1$ for timelike geodesics. From the Hamilton's equation $dx^\mu/d\tau = \partial\mathcal{H}/\partial\pi_\mu$, one obtains the constants of motion,

$$
E = -\pi_t = -g_{tt} \dot{t} - g_{t\phi} \dot{\phi} + q A_t, \qquad (32)
$$

$$
L = \pi_\phi = g_{t\phi} \dot{t} + g_{\phi\phi} \dot{\phi} - q A_\phi. \qquad (33)
$$

In order to determine the additional constant of motion, i.e., the Carter constant $\mathcal{C}$ [25], the Hamilton-Jacobi equation

$$
-2 \frac{\partial \mathcal{S}}{\partial \tau} = g^{\mu\nu} \left(\frac{\partial \mathcal{S}}{\partial x^\mu} + q A_\mu\right) \left(\frac{\partial \mathcal{S}}{\partial x^\nu} + q A_\nu\right), \qquad (34)
$$

must be solved. The components A_μ are given by (19). The charge of the test particle will also be screened. In terms of A_t, (34) can be reduced to

$$
\begin{aligned}
-2 \frac{\partial \mathcal{S}}{\partial \tau} = &-\frac{1}{\Sigma\Delta} \left\{ (r^2 + a^2) \frac{\partial \mathcal{S}}{\partial t} + a \frac{\partial \mathcal{S}}{\partial \phi} + q \Sigma A_t \right\}^2 \\
&+ \frac{1}{\Sigma \sin^2\theta} \left\{ a \sin^2\theta \frac{\partial \mathcal{S}}{\partial t} + \frac{\partial \mathcal{S}}{\partial \phi} \right\}^2 \\
&+ \frac{1}{\Sigma} \left\{ \Delta \left(\frac{\partial \mathcal{S}}{\partial r}\right)^2 + \left(\frac{\partial \mathcal{S}}{\partial \theta}\right)^2 \right\}. \qquad (35)
\end{aligned}
$$

In order to get the screened value of the test charge we require

$$
\begin{aligned}
q \Sigma A_t &= \left\{ 1 - \frac{10\alpha}{225\pi} D_Q^2 + \frac{10\alpha}{225\pi} H_Q^2 + \frac{60\alpha}{225\pi} H_Q^2 \frac{H_Q^2}{D_Q^2} \right\} q Q r, \\
&= \tilde{q} \, \tilde{Q} \, r, \qquad (36)
\end{aligned}
$$

where $\tilde{Q}$ is the screened black hole charge (27), and $\tilde{q}$ is the screened charge of the test particle

$$
\begin{aligned}
\tilde{q}^2 = q^2 \Bigg\{ 1 - \frac{5\alpha}{225\pi} \Bigg[3D_Q^2 + 4H_Q^2 \left(1 - \frac{a^2 \cos^2\theta}{\Sigma}\right) \\
\times \left(13 - 12 \frac{a^2 \cos^2\theta}{\Sigma} + 12 \frac{a^4 \cos^4\theta}{\Sigma^4}\right) \Bigg] \Bigg\}, \qquad (37)
\end{aligned}
$$

which depends on D_Q and H_Q. It is induced by the electric field generating the clouds of virtual charges.

In order to be able to separate variables, we use the separation ansatz

$$
\mathcal{S} = \frac{1}{2} \mu^2 \tau - E t + L \phi + S_r(r) + S_\theta(\theta), \qquad (38)
$$

with the constants of motion μ, E, and L. The solutions for S_r and S_θ read

$$S_r(r) = \int^r \frac{\sqrt{R(r)}}{\Delta} dr, \qquad S_\theta(\theta) = \int^\theta \sqrt{\Theta(\theta)} d\theta, \tag{39}$$

where the functions R, $\mathcal{P}$, and Θ are defined by

$$R(r) \equiv \mathcal{P}^2(r) - \Delta(\mu^2 r^2 + K), \tag{40}$$

$$\mathcal{P}(r) \equiv (r^2 + a^2)E - aL - \tilde{q}\,\tilde{Q}\,r, \tag{41}$$

$$\Theta(\theta) \equiv \mathcal{C} - [L^2 \csc^2\theta + a^2(\mu^2 - E^2)]\cos^2\theta, \tag{42}$$

with the modified Carter constant $K \equiv \mathcal{C} + [L - aE]^2$. In this way, the equations of motion become

$$\Sigma\dot{t} = \frac{(r^2 + a^2)}{\Delta}\mathcal{P}(r) + a\{L - aE\sin^2\theta\}, \tag{43}$$

$$(\Sigma\dot{r})^2 = R(r), \tag{44}$$

$$(\Sigma\dot{\theta})^2 = \Theta(\theta), \tag{45}$$

$$\Sigma\dot{\phi} = \frac{a}{\Delta}\mathcal{P}(r) + \frac{\{L - aE\sin^2\theta\}}{\sin^2\theta}. \tag{46}$$

These equations of motion are equivalent to those for the KN case, with the charges replaced by the screened charges (27) and (37). The complete description of the charged particle motion in KN spacetimes, as well as the analytical solutions in terms of Weierstrass elliptic functions, were presented in detail by Hackmann *et al.* [26]. Their solutions and classification can be taken over for the EEH case by replacing Q and q with $\tilde{Q}$ and $\tilde{q}$.

The turning point of an orbit is given by the condition $\dot{r} = 0$, which from (44) corresponds to $R = 0$. Following Grunau *et al.* [27], one defines the effective potential as solution of the quadratic polynomial in E, i.e.,

$$0 = (\Sigma\dot{r})^2 = R(r) = (E - V^+_{\rm eff})(E - V^-_{\rm eff}), \tag{47}$$

with

$$V^\pm_{\rm eff} = \frac{1}{(r^2 + a^2)}\left[aL + \tilde{q}\,\tilde{Q}\,r \pm \sqrt{(\mu^2 r^2 + K)\Delta}\right]. \tag{48}$$

If the charges have the same sign, $\tilde{q}\,\tilde{Q} > 0$, then the effective potential $V^+_{\rm eff}$ is always positive. For $\tilde{q}\,\tilde{Q} < 0$,

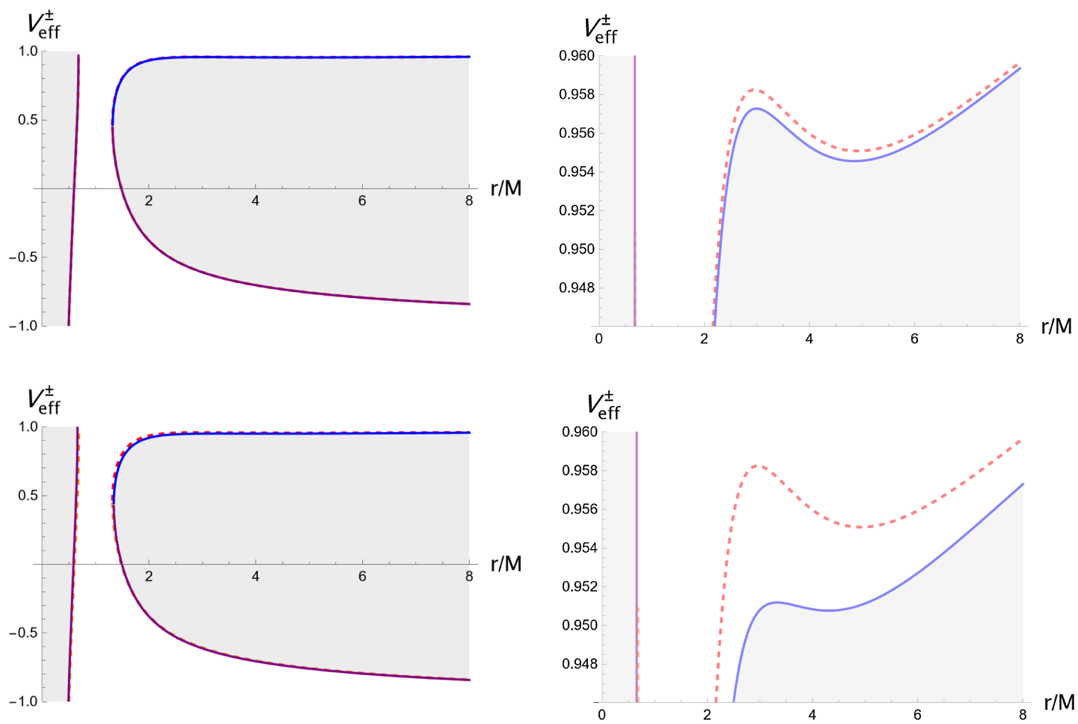

FIG. 1. The potentials $V^\pm_{\rm eff}$ as a function of r/M for the KN case (dashed line) and the rotating EEH one (continuous line). The figure on the rhs shows the enlargement of the corresponding region of the figure on the lhs. For the figures on the top, $\tilde{q}$ is the screened value at the radius of the minimum of the KN potential, while for those on the bottom, $\tilde{q}$ is the screened value at the maximum. The EH effect at the maximum is more visible since it lays at a smaller value of r. The other parameters are $M = 1 \times 10^4 M_\odot$, $Q = 0.9M$, $a = 0.3M$, $\mu = 1$, $L = 0.8M$, $K = 4M^2$, and $q = 0.5$.

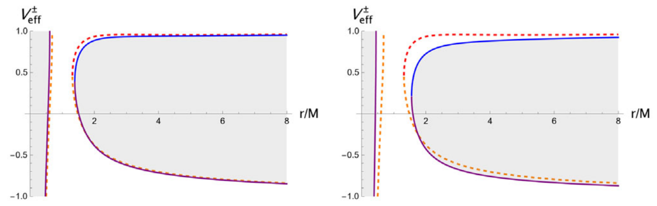

FIG. 2. The potentials $V_{\rm eff}^{\pm}$ as a function of r/M for the KN case (dashed line) and the EEH one (continuous line), with $\tilde{q}$ the screened value at the minimum of the KN potential. For the figure on the lhs, $M = 2\times 10^3 M_{\odot}$, while for that on the rhs, $M = 1\times 10^3 M_{\odot}$. Due to the screening effect on the charges, there is no maxima and minima. The other parameters are $Q = 0.9M$, $a = 0.3M$, $\mu = 1$, $L = 0.8M$, $K = 4M^2$, and $q = 0.5$.

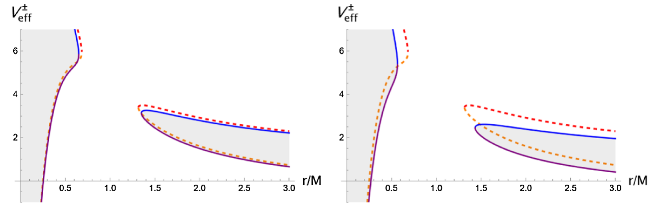

FIG. 3. The potentials $V_{\rm eff}^{\pm}$ as a function of r/M for the KN case (dashed line) and the EEH one (continuous line), with $\tilde{q}$ the screened value at the minimum of the KN potential and for a bigger value of the test charge $q = 5$. For the figure on the lhs, $M = 4\times 10^4 M_{\odot}$, while for that on the rhs, $M = 2\times 10^4 M_{\odot}$. The other parameters are $Q = 0.9M$, $a = 0.3M$, $\mu = 1$, $L = 0.8M$, and $K = 4M^2$.

both effective potentials $V_{\rm eff}^{\pm}$ may take negative values, which corresponds to negative values of the energy. At infinity, the limit value of the effective potential is given by $\lim_{r\to\infty} V_{\rm eff}^{\pm} = \pm 1$.

Both effective potentials $V_{\rm eff}^{\pm}$ coincide at the horizons $r_{\pm}$ where $\Delta = 0$. The event horizon r_+ bounds an inner region incommunicable to an asymptotically flat world outside [28], and, in principle, a particle crossing the horizon would migrate to a different world. Nevertheless, the region between the two horizons, $r_- < r < r_+$, is not part of the domain of (48), since here $\Delta < 0$, which also implies that $R > 0$. There cannot be any turning points between the horizons, and there is a turning point at a horizon only if $\mathcal{P}(r_{\pm}) = 0$.

Figures 1 to 3 combine both effective potentials $V_{\rm eff}^{\pm}$ as functions of r for different values of the parameters. The gray areas mark physically forbidden regions. There is a potential barrier located in the interval $0 < r \leq r_-$, while outside the event horizon, in the region $r > r_+$, the existence of maxima and minima of the potential implies the possibility for stable and unstable bound orbits. An example is given in Fig. 1.

Due to the screening of the test charge, the EEH effective potential lays below the KN one, as can also be seen in Fig. 1. If there is a charged test particle reaching a bound orbit in the region near the minimum of the KN potential and virtual charges are generated by the charge of the black hole, then the test charge will follow the orbit described by the EEH spacetime, with both $\tilde{q}$ and $\tilde{Q}$ being the screened values at the radius of this minimum. Something similar would happen if the test charge reaches the maximum, but the effect would be increased.

The screening on the effective potential for different values of the mass M of the black hole is presented in Figs. 2 and 3. The effect is more visible for smaller values of M. The potential can be lowered enough such that the maximum and minimum of the potential disappear. In this case, the test charge would not reach a bound orbit outside the event horizon. The latter is shown in Fig. 2. An example for a bigger value of the test charge is given in Fig. 3.

V. THE LIGHT GEODESICS

In linear Maxwell-Lorentz electrodynamics, the discontinuities of the field propagate according to the equation for the characteristic surfaces, $g^{\mu\nu}S_{,\mu}S_{,\nu} = 0$, which in standard optics is known as an eikonal equation. The corresponding linear photons travel along null geodesics of the geometrical metric $g_{\mu\nu}$.

In EH NLED, photons propagate along null geodesics of the effective Plebański pseudometric $\gamma_{\mu\nu}$ [18] given by

$$\gamma^{\mu\nu} = g^{\mu\nu} + \frac{80\alpha}{225 D_c^2} T^{\mu\nu}, \tag{49}$$

which differs from the geometrical metric $g_{\mu\nu}$, since it contains the energy-momentum tensor as well. The propagation equation for the nonlinear electromagnetic field discontinuities reads

$$\gamma^{\mu\nu} S_{,\mu} S_{,\nu} = 0, \tag{50}$$

where $S_{,\mu}$ are the normal vectors to the characteristic surface S. Therefore, the energy-momentum tensor $T_{\mu\nu}$ of the EH nonlinear field is responsible for the fact that these surfaces are not null surfaces of the geometrical metric.

A. The equations of motion

The null trajectories of nonlinear photons are then obtained from the Hamilton-Jacobi equation

$$\frac{\partial S}{\partial \tau} = -\frac{1}{2}\gamma^{\mu\nu}\frac{\partial S}{\partial x^{\mu}}\frac{\partial S}{\partial x^{\nu}}, \tag{51}$$

written in terms of the effective Plebański pseudometric (49). It is proposed a Hamilton function with the form of (38), and the constants of motion E, L, and $\mathcal{C}$. For light rays, the normalizing condition reads $\mu^2 = -\gamma_{\mu\nu}\dot{x}^{\mu}\dot{x}^{\nu} = 0$, for null geodesics. The separation of variables for the Hamilton-Jacobi equation results in the solutions

$$S_r(r) = \int^r \left[1 + \frac{10\alpha}{225\pi} D_Q^2\right] \frac{\sqrt{R(r)}}{\Delta} dr, \tag{52}$$

$$S_\theta(\theta) = \int^\theta \sqrt{\Theta(\theta)} d\theta, \tag{53}$$

where the light rays functions R, $\mathcal{P}$, and Θ are defined by

$$R(r) \equiv \left[1 - \frac{20\alpha}{225\pi} D_Q^2\right] \mathcal{P}^2(r) - K\Delta, \tag{54}$$

$$\mathcal{P}(r) \equiv (r^2 + a^2)E - aL, \tag{55}$$

$$\Theta(\theta) \equiv \mathcal{C} - [L^2 \csc^2\theta - a^2E^2]\cos^2\theta. \tag{56}$$

Again we introduce a modified Carter constant $K \equiv \mathcal{C} + [L - aE]^2$. Then the equations of motion read

$$\Sigma\dot{t} = \left[1 - \frac{10\alpha}{225\pi} D_Q^2\right] \frac{(r^2 + a^2)}{\Delta} \mathcal{P}(r) + \left[1 + \frac{10\alpha}{225\pi} D_Q^2\right] a\{L - aE\sin^2\theta\}, \tag{57}$$

$$(\Sigma\dot{r})^2 = R(r), \tag{58}$$

$$(\Sigma\dot{\theta})^2 = \left[1 + \frac{20\alpha}{225\pi} D_Q^2\right] \Theta(\theta), \tag{59}$$

$$\Sigma\dot{\phi} = \left[1 - \frac{10\alpha}{225\pi} D_Q^2\right] \frac{a}{\Delta} \mathcal{P}(r) + \left[1 + \frac{10\alpha}{225\pi} D_Q^2\right] \frac{\{L - aE\sin^2\theta\}}{\sin^2\theta}. \tag{60}$$

These equations differ from those for massless particles, namely (43)–(46), for $\mu = 0$ and $q = 0$. It is worthwhile to mention the fact that the Hamilton-Jacobi equation can be completely separated for EH quasiconstant fields. The electric field $D_Q \equiv Q^2/(D_c^2\Sigma^2)$ is considered as a constant on the photon region.

From (58) we obtain the conditions under which the light rays reach the photon region at $r = r_c$, i.e., $\dot{r} = 0$ and $\ddot{r} = 0$, which correspond to the conditions $R(r_c) = 0$ and $R'(r_c) = 0$. Under these conditions, the constants $\eta \equiv L/E$ and $\chi \equiv \mathcal{C}/E^2$ are given by

$$\eta = \frac{r_c^3 - 3Mr_c^2 + (a^2 + 2\tilde{Q}_c^2)r_c + Ma^2}{a(M - r_c)}, \tag{61}$$

$$\chi = \frac{r_c^2}{a^2(r_c - M)^2} \left[4Mr_c(a^2 + \tilde{Q}_c^2) - 4\tilde{Q}_c^2\Delta_c - r_c^2(r_c - 3M)^2 - \frac{20\alpha}{225\pi} D_Q^2(\Sigma_{c_{\mathrm{KN}}})(4a^2\Delta_c)\right], \tag{62}$$

where $\Delta_c = r_c^2 + a^2 - 2Mr_c + \tilde{Q}_c^2$. The screening of the charge is evaluated at the radial distance of the KN photon region $r_{c_{\mathrm{KN}}}$

$$\tilde{Q}_c^2 = Q^2\left\{1 - \frac{5\alpha}{225\pi}\left[D_Q^2(\Sigma_{c_{\mathrm{KN}}}) - 4H_Q^2(\Sigma_{c_{\mathrm{KN}}}) \times \left(7 - 12\frac{a^2\cos^2\theta_{c_{\mathrm{KN}}}}{\Sigma_{c_{\mathrm{KN}}}} + 12\frac{a^4\cos^4\theta_{c_{\mathrm{KN}}}}{\Sigma_{c_{\mathrm{KN}}}^2}\right) \times \left(1 - \frac{a^2\cos^2\theta_{c_{\mathrm{KN}}}}{\Sigma_{c_{\mathrm{KN}}}}\right)\right]\right\}, \tag{63}$$

where the electric field $D_Q(\Sigma_{c_{\mathrm{KN}}}) = Q^2/(D_c^2\Sigma_{c_{\mathrm{KN}}}^2)$, the magnetic one $H_Q(\Sigma_{c_{\mathrm{KN}}}) = \mathcal{M}^2\cos^2\theta_{c_{\mathrm{KN}}}/(D_c^2\Sigma_{c_{\mathrm{KN}}}^3)$, and $\Sigma_{c_{\mathrm{KN}}} = r_{c_{\mathrm{KN}}}^2 + a^2\cos^2\theta_{c_{\mathrm{KN}}}$. From (61) we obtain the polynomial of third order

$$r_c^3 - 3Mr_c^2 + \left[a(a + \eta) + 2\tilde{Q}_c^2\right] r_c + aM(a - \eta) = 0. \tag{64}$$

It has either three real roots or one real root and two complex roots. The real roots can have multiplicity two or three, and be either positive or negative. Following Cardano's method, we determine the values of the parameters for which the polynomial has positive real zeros. The exact solutions read

$$\begin{aligned}
&\mathcal{A} > 0, \quad \mathcal{B} \le 1: r_c = M + 2\sqrt{\mathcal{A}}\cos\left(\frac{1}{3}\cos^{-1}\mathcal{B}\right),\\
&\mathcal{A} > 0, \quad \mathcal{B} > 1: r_c = M + 2\sqrt{\mathcal{A}}\cosh\left(\frac{1}{3}\cosh^{-1}\mathcal{B}\right),\\
&\mathcal{A} < 0: \ r_c = M - 2\sqrt{|\mathcal{A}|}\sinh\left(\frac{1}{3}\sinh^{-1}|\mathcal{B}|\right),
\end{aligned} \tag{65}$$

where the functions $\mathcal{A}$ and $\mathcal{B}$ are defined by

$$\mathcal{A} \equiv M^2 - \frac{1}{3}\left[a(a + \eta) + 2\tilde{Q}_c^2\right], \tag{66}$$

$$\mathcal{B} \equiv M\left(M^2 - a^2 - \tilde{Q}_c^2\right)\mathcal{A}^{-3/2}. \tag{67}$$

Besides the black hole parameters, they depend on the constant η only. Thus, after substituting the solutions (65) into (62), we obtain a parametric function $\chi(\eta)$. This method was introduced by Cunha and Herdeiro [29].

B. The shadow of the black hole

Following Bardeen *et al.* [30], we have to consider a set of local observers who "rotate with the geometry," called locally nonrotating frames (LNRFs). The observer's worldlines are perpendicular to the hypersurfaces $t = t_0$, and his/her coordinates are $r = r_0$, $\theta = \theta_0$, and $\phi = \omega t + \phi_0$, where t_0, r_0, θ_0, and ϕ_0 are constants. Each observer has his/her locally Minkowskian coordinate basis, an orthonormal tetrad. In the case of an axially symmetric spacetime (26), the tetrad for the LNRF is given by

$$\mathbf{e}_{(t)} = \sqrt{-g^{tt}}\frac{\partial}{\partial t} - \frac{g^{t\phi}}{\sqrt{-g^{tt}}}\frac{\partial}{\partial \phi},$$
$$\mathbf{e}_{(r)} = \sqrt{g^{rr}}\frac{\partial}{\partial r}, \qquad \mathbf{e}_{(\theta)} = \sqrt{g^{\theta\theta}}\frac{\partial}{\partial \theta},$$
$$\mathbf{e}_{(\phi)} = \sqrt{g^{\phi\phi} - \frac{(g^{t\phi})^2}{g^{tt}}}\frac{\partial}{\partial \phi}. \tag{68}$$

In this case, since the tetrad is carried by the observer, the geometrical metric has to be used. The Boyer-Lindquist components of the LNRF basis vector are given by $e_{(i)} = e^{\mu}_{(i)}\frac{\partial}{\partial x^{\mu}}$.

Since in NLED the momentum of the light rays is calculated by means of the effective Plebański pseudometric (49), we have $p_\mu = \gamma_{\mu\nu}\dot{x}^\nu$. Hence, on this basis the momentum is obtained from

$$\mathbf{p}^{(i)} = \eta^{(i)(j)} e^{\mu}_{(j)}\gamma_{\mu\nu}\dot{x}^{\nu}, \tag{69}$$

where $\eta^{(i)(j)} = \mathrm{diag}\{-1, 1, 1, 1\}$ is the Minkowski metric. The celestial coordinates in the image plane seen by an observer are given by $(x, y) = (-r\mathbf{p}^{(\phi)}/\mathbf{p}^{(t)}, r\mathbf{p}^{(\theta)}/\mathbf{p}^{(t)})_0$, where the sign on x stands for a black hole rotating from left to right as seen by the observer [31], and where the subindex zero denotes the observer's location (r_0, θ_0). For distant observers, $r_0 \to \infty$, they can be reduced to

$$x = -\frac{\eta}{\sin\theta_0}, \tag{70}$$

$$y = \sqrt{\chi - (\eta^2 \csc^2\theta_0 - a^2)\cos^2\theta_0}. \tag{71}$$

If the angular position of the observer θ_0 is known, then from (70) one obtains a function $\eta(x)$ that, via (65) and (62), allows us to reparametrize the celestial coordinate $y(x) = \sqrt{\chi(x) - (x^2 - a^2)\cos^2\theta_0}$. This parametrized function has the same form as the one for the linear case.

Since (26) corresponds to a KN solution with screened charge, one may expect that the EEH shadow is equivalent to that of KN for a smaller black hole charge. This is not the case since there is an additional nonlinear contribution to the parametrized equation for the black hole shadow, coming from the last term in (62). It is the most important contribution and arises from the fact that the light propagates along null geodesics of the effective Plebański pseudometric (49), namely, from considering that the vacuum is endowed with an effective dielectric constant.

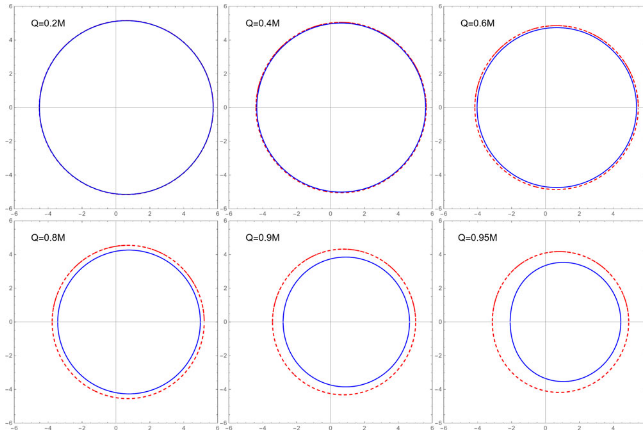

FIG. 4. The shadow of the EEH rotating black hole (continuous line) and that of KN (dashed line), for different values of Q. As Q increases, the EEH nonlinear effect becomes more visible. The parameters are $M = 1 \times 10^4 M_\odot$, $a = 0.3M$, and $\theta_0 = \pi/2$.

The photon orbits and the shadow for the static case, i.e., for a screened Reissner-Nordström black hole, were analyzed in [32], while those in the KN case were studied for example in [33].

One has to keep in mind that Bardeen's approach is only appropriate for observers at large distances. The celestial coordinates or impact parameters, (70) and (71), have the dimension of a length, and have to be divided by r_0 in order to be identified as the measured angles in the observer's sky [34]. In the following figures, the impact parameters x and y, will be written in units of the black hole mass M. Figure 4 displays the shadow of the EEH rotating black hole for fixed mass and angular momentum, and varying the charge. The black hole parameters satisfy the event horizon condition $a^2 + \tilde{Q}^2 \leq M^2$. The EEH nonlinear terms depend on $\tilde{Q}$ since they include the electromagnetic fields D_Q and H_Q defined by (20). As expected, for bigger values of $\tilde{Q}$ the EH effect becomes more visible.

When studying the KN case, a smaller charge Q would result on a bigger size of the shadow. This can also be seen from Fig. 4, in which the KN shadow (dashed line) for $Q = 0.2M$ is bigger than that for $Q = 0.8M$, for instance. The EEH charge is screened, i.e., $\tilde{Q} < Q$. Thus, one would expect the EEH shadow to be bigger than the KN one, which is not the case. The latter results from the fact that the EH theory endows the vacuum with an effective dielectric constant, as mentioned above. Hence, the light propagates in this medium described by the effective pseudometric $\gamma_{\mu\nu}$, and additional EH nonlinear terms arise, e.g., the last term of (62). The photon propagation in this medium is the responsible for the EEH shadow to lay inside the KN one.

Figure 5 shows the EEH shadow for different masses and for fixed parameters Q/M and a/M. For bigger values of M, the effect is not visible, but for smaller values of M the effect becomes relevant. For a fixed Q/M, the effect

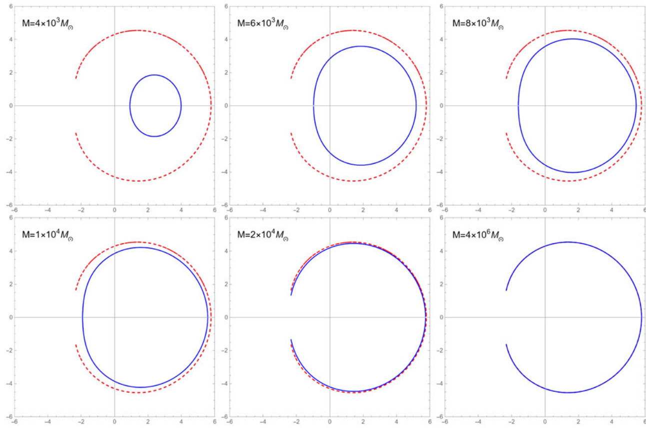

FIG. 5. The shadow of the EEH rotating black hole (continuous line) and that of KN (dashed line), for different values of M. As M decreases, the EEH nonlinear effect becomes more relevant. The parameters are $Q = 0.8M$, $a = 0.6M$, and $\theta_0 = \pi/2$.

vanishes for big masses. The same happens in the static case [19]. This would suggest that for supermassive black holes, the EH effect on the photons propagation is not visible. One can understand this fact by analyzing the dimensions of the quantum corrections, all of which are proportional to $\frac{\alpha}{225\pi} D_Q^2(\Sigma_{c_{\mathrm{KN}}})$. For instance, in the static case it reads $\frac{\alpha}{225\pi D_c^2} \frac{(Q/M)^2}{(r_{c_{\mathrm{KN}}}/M)^4} \frac{1}{M^2}$, where the parameter $0 \leq |Q|/M \leq 1$ is restricted by the event horizon condition, and $r_{c_{\mathrm{KN}}}/M = 3\left(1 + \sqrt{1 - 8Q^2/(9M^2)}\right)/2$ can only take values between $2 \leq r_{c_{\mathrm{KN}}}/M \leq 3$; the remaining factor $1/M^2$ is responsible for the dimension of the quantum corrections. Hence, for bigger masses the EH effects are smaller.

The quantum effect on the shadow of the EEH rotating black hole depends on the value of M, Q, and of the screening, as in the static case. In the latter, considering small values of Q would completely reduce the EH effect on the shadow, which would then approach to the shadow of the Schwarzschild solution. Nevertheless, in the rotating case the EH effect additionally depends on the angular momentum a of the black hole. This can be seen from the last term of (62). One may consider very small values of Q, but together with small values of M and nonzero values of a, such that the effect on the shadow is still visible. The latter is shown in Fig. 6, which displays the shadow for fixed M and Q, and varying a. As a increases, the EEH nonlinear effect on the shadow grows.

For astrophysical black holes one does not expect big charges, but the charge of a black hole may be different

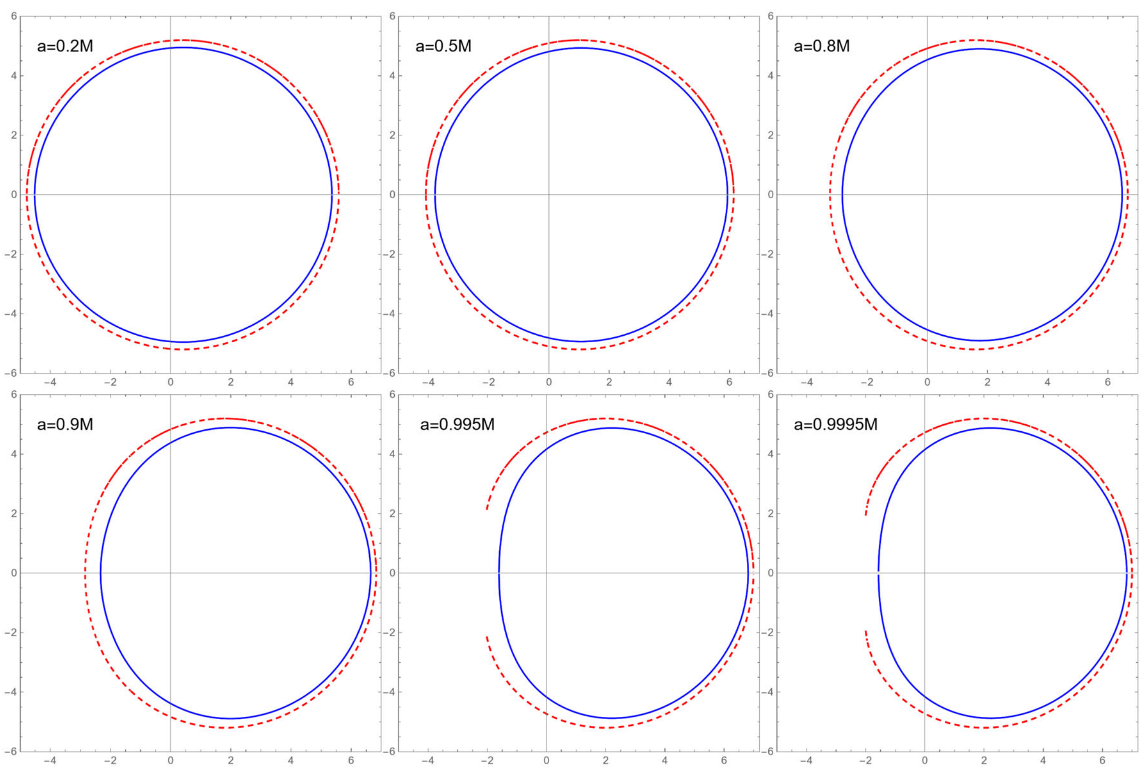

FIG. 6. The shadow of the EEH rotating black hole (continuous line) and that of KN (dashed line), for nonvanishing values of a. Even for a small fixed value of $Q = 5 \times 10^{-4} M$ the EEH nonlinear effect is still visible, due to the nonlinear contribution depending on the angular momentum a, (62). The mass corresponds to that for a stellar black hole, $M = 5\,M_\odot$. The parameters satisfy the condition $a^2 + \tilde{Q}^2 \leq M^2$. The angle $\theta_0 = \pi/2$.

from zero during the accretion of charged matter like plasma. Moreover, during the gravitational collapse of a star to a black hole, processes of charge separation and consequent pair production by vacuum polarization occur. The black holes formed by collapsing stars are the stellar black holes, with masses within a few solar masses above the critical mass of neutron stars, $M > 3.2M_{\odot}$. Hence, for a stellar black hole the EH effect on the light propagation becomes relevant as long as it spins and even for a very small charge, as that in Fig. 6.

VI. SUMMARY AND CONCLUSIONS

QED vacuum corrections to the Maxwell-Lorentz theory can be accounted for by the effective QED theory after one loop of nonperturbative quantization, i.e., the EH NLED [1]. The vacuum is treated as a specific type of medium, the polarizability and magnetizability properties of which are determined by clouds of virtual charges surrounding the real charges and currents, this fact can be interpreted as a kind of dielectric constant of the vacuum.

The EEH generalization of the KN black hole solution was recently performed by Bretón *et al.* [20]. They considered the QED interpretation of the EH NLED and generated a rotating electrically charged black hole solution by assuming that the nonlinearity influence only the electric charge by means of a screening of it. The geometry is only affected through the screened values of the real charges and of the induced magnetic dipole moment. The black hole solution is then interpreted as a screened KN one, as it happens for the static solution, which is considered as screened Reissner-Nordström one [15,19].

We first studied the geodesics of massive charged test particles, which interaction with the electric field is described by means of the electromagnetic potential A_μ. The A_μ is obtained by using the material relations of the EH NLED. When solving the Hamilton-Jacobi equation, we find the screening of the test particle charge. Hence, the features of the charged particle motion in a KN spacetime [26] are recovered. The screening effect causes the test charge to follow a different kind of orbit than the one predicted in the KN case.

The size and the shape of the shadow depend on the properties of the regions through which light travels [34]. Hence, we study the light trajectories by means of the effective Plebański pseudometric [18], which contains the energy-momentum tensor of the EH NLED theory. The Hamilton-Jacobi equation is solved in the framework of the EEH theory and the null geodesic equations are presented. We solve the conditions under which light rays reach the photon region and obtain a parametric function relating the constants of motion. We also analyze the shadow of the black hole measured by a distant observer. The shadow barely shrinks when we consider the EH effects, i.e., the EEH rotating black hole shadow lays always inside the shadow of the KN black hole.

Astrophysical black holes are not expected to carry big charges. In the static case [19], small values of the charge would lead to extremely small visibility of the EH effects. Nevertheless, in the rotating case there is a nonlinear contribution depending on the angular momentum of the black hole. For small charges and small masses, of the order of stellar black holes, the EH effect on the shadow would become relevant. As in the static case, the nonlinear effect is not visible for large masses, like those from supermassive black holes.

The charge of a black hole may be different to zero in some accretion scenarios and during the gravitational collapse of a star to a black hole. In the latter, processes of charge separation and consequent pair production by vacuum polarization occur [7]. The black holes formed by collapsing stars are the stellar black holes, for which the EH effects on the light propagation should be considered. Although presently the observation of the shadow of stellar black holes is not viable, it would provide further insights on the aspects of nuclear physics and electrodynamics in strong gravitational fields, in combination with other observational programs, such as x-ray heat maps and gamma ray bursts.

One additional issue remains to be considered in order to study all the consequences of the screened Kerr-Newman-like solution [20], i.e., the thermodynamics [35–37] associated with the mentioned black hole solution and the energy dissipation at the horizon [38,39]. This work is in progress and will be reported elsewhere.

ACKNOWLEDGMENTS

D. A. acknowledges financial support from DAAD fellowship Ref. No. : 91832671. C. L. is supported by the Deutsche Forschungsgemeinschaft (DFG, German Research Foundation) under Germany's Excellence Strategy-EXC-2123 "QuantumFrontiers"—Grant No. 390837967, the CRC 1464 "Relativistic and Quantum-based Geodesy" (TerraQ), and by the Research Training Group GRK1620 "Models of Gravity."

[1] W. Heisenberg and H. Euler, Folgerungen aus der Diracschen Theorie des Positrons, Z. Phys. **98**, 714 (1936).
[2] S. Weinberg, *The Quantum Theory of Fields* (Cambridge University Press, Cambridge, England, 1995), Vol. 2.
[3] J. Schwinger, On gauge invariance and vacuum polarization, Phys. Rev. **82**, 664 (1951).
[4] F. W. Hehl and Y. N. Obukhov, *Foundations of Classical Electrodynamics: Charge, Flux, and Metric* (Springer Science and Business Media, New York, 2003), Vol. 33.
[5] G. Boillat, Nonlinear electrodynamics: Lagrangians and equations of motion, J. Math. Phys. (N.Y.) **11**, 941 (1970).
[6] G. Brodin, M. Marklund, and L. Stenflo, Proposal for Detection of QED Vacuum Nonlinearities in Maxwell's Equations by the Use of Waveguides, Phys. Rev. Lett. **87**, 171801 (2001).
[7] R. Ruffini, G. Vereshchagin, and S.-S. Xue, Electron–positron pairs in physics and astrophysics: From heavy nuclei to black holes, Phys. Rep. **487**, 1 (2010).
[8] R. Ruffini, R. Moradi, J. A. Rueda, L. Becerra, C. Bianco, C. Cherubini, S. Filippi, Y. Chen, M. Karlica, N. Sahakyan *et al.*, On the GeV emission of the type I BdHN GRB 130427A, Astrophys. J. **886**, 82 (2019).
[9] J. Rueda and R. Ruffini, The blackholic quantum, Eur. Phys. J. C **80**, 300 (2020).
[10] J. Rueda and R. Ruffini, The quantum emission of an alive black hole, Int. J. Mod. Phys. D **30**, 2141003 (2021).
[11] J. Rueda, R. Ruffini, and R. Kerr, Gravitomagnetic interaction of a Kerr black hole with a magnetic field as the source of the jetted GeV radiation of gamma-ray bursts, Astrophys. J. **929**, 56 (2022).
[12] R. Genzel, F. Eisenhauer, and S. Gillessen, The galactic center massive black hole and nuclear star cluster, Rev. Mod. Phys. **82**, 3121 (2010).
[13] E. A. Abbott, B. P. (LIGO Scientific Collaboration and Virgo Collaboration), Observation of Gravitational Waves from a Binary Black Hole Merger, Phys. Rev. Lett. **116**, 061102 (2016).
[14] The Event Horizon Telescope Collaboration *et al.*, First M87 Event Horizon Telescope Results. I. The Shadow of the Supermassive Black Hole, Astrophys. J. Lett. **875**, L1 (2019).
[15] R. Ruffini, Y.-B. Wu, and S.-S. Xue, Einstein-Euler-Heisenberg theory and charged black holes, Phys. Rev. D **88**, 085004 (2013).
[16] H. Yajima and T. Tamaki, Black hole solutions in Euler-Heisenberg theory, Phys. Rev. D **63**, 064007 (2001).
[17] M. Born, L. Infeld, and R. H. Fowler, Foundations of the new field theory, Proc. R. Soc. A **144**, 425 (1934).
[18] J. F. Plebański, *Lectures on Nonlinear Electrodynamics* (Nordita, Copenhagen, 1970).
[19] D. Amaro and A. Macías, Geodesic structure of the Euler-Heisenberg static black hole, Phys. Rev. D **102**, 104054 (2020).
[20] N. Bretón, C. Lämmerzahl, and A. Macías, Rotating structure of the Euler-Heisenberg black hole, Phys. Rev. D **105**, 104046 (2022).
[21] G. Gibbons and C. A. R. Herdeiro, The Melvin universe in Born-Infeld theory and other theories of nonlinear electrodynamics, Classical Quantum Gravity **18**, 1677 (2001).
[22] H. Salazar, A. García, and J. Plebański, Duality rotations and type D solutions to Einstein equations with nonlinear electromagnetic sources, J. Math. Phys. (N.Y.) **28**, 2171 (1987).
[23] K. S. Thorne, C. W. Misner, and J. A. Wheeler, *Gravitation* (Freeman, San Francisco, CA, 2000).
[24] H. Goldstein, C. Poole, and J. Safko, *Classical Mechanics* (Addison Wesley, New York, 2002).
[25] B. Carter, Global structure of the Kerr family of gravitational fields, Phys. Rev. **174**, 1559 (1968).
[26] E. Hackmann and H. Xu, Charged particle motion in Kerr-Newmann space-times, Phys. Rev. D **87**, 124030 (2013).
[27] S. Grunau and V. Kagramanova, Geodesics of electrically and magnetically charged test particles in the Reissner-Nordström space-time: Analytical solutions, Phys. Rev. D **83**, 044009 (2011).
[28] S. Chandrasekhar, *The Mathematical Theory of Black Holes* (Oxford University Press, New York, 1983).
[29] P. Cunha and C. Herdeiro, Shadows and strong gravitational lensing: A brief review, Gen. Relativ. Gravit. **50**, 42 (2018).
[30] J. M. Bardeen, W. H. Press, and S. A. Teukolsky, Rotating black holes: Locally nonrotating frames, energy extraction, and scalar synchrotron radiation, Astrophys. J. **178**, 347 (1972).
[31] J. M. Bardeen, Timelike and null geodesics in the Kerr metric, in *Proceedings of: Les Houches Summer School of Theoretical Physics 1972*, edited by C. DeWit and B. S. DeWit, (Gordon and Breach, NY, 1973), pp. 215–240, https://inspirehep.net/literature/1357064.
[32] D. Amaro and A. Macías, Exact lens equation for the Einstein-Euler-Heisenberg static black hole, Phys. Rev. D **106**, 064010 (2022).
[33] A. de Vries, The apparent shape of a rotating charged black hole, closed photon orbits and the bifurcation set A4, Classical Quantum Gravity **17**, 123 (2000).
[34] V. Perlick and O. Y. Tsupko, Calculating black hole shadows: Review of analytical studies, Phys. Rep. **947**, 1 (2022).
[35] P. Davies, The thermodynamic theory of black holes, Proc. R. Soc. A **353**, 499 (1977).
[36] P. Wang, H. Wu, and H. Yang, Thermodynamics of nonlinear electrodynamics black holes and the validity of weak cosmic censorship at charged particle absorption, Eur. Phys. J. C **79**, 572 (2019).
[37] O. Ruiz, U. Molina, and P. Viloria, Thermodynamic analysis of Kerr-Newman black holes, J. Phys. Conf. Ser. **1219**, 012016 (2019).
[38] A. Peltola and J. Mäkelä, Radiation of the inner horizon of the Reissner-Nordström black hole, Int. J. Mod. Phys. D **15**, 817 (2006).
[39] T. Damour and R. Ruffini, Black-hole evaporation in the Klein-Sauter-Heisenberg-Euler formalism, Phys. Rev. D **14**, 332 (1976).